Synthesis and Characterization of the Phosphorus Halide–Boron Halide Complexes X_3PBY_3 (X = Cl, Br, I; Y = Br, I) by ^{31}P MAS NMR, IR, and Raman Spectroscopy and the Crystal Structure of Br_3PBBr_3

Christoph Aubauer,[a] Günter Engelhardt,[b] Thomas M. Klapötke,*[a] Heinrich Nöth,[a][+] Axel Schulz,[a] and Marcus Warchhold[a][+]

Keywords: Density functional calculations / Phosphorus / Boron / Halides / NMR spectroscopy / Raman spectroscopy

The phosphorus halide–boron halide complexes X_3PBY_3 (X = Cl, Br, I; Y = Br, I) were prepared and characterized by Raman and IR spectroscopy. Density functional theory (B3LYP) was applied to calculate structural and vibrational data. Assignments of the vibrational normal modes for these Lewis acid–base adducts were made on the basis of their Raman and IR spectra in comparison with computational results. The compounds Cl_3PBBr_3, Br_3PBBr_3, I_3PBBr_3, and I_3PBI_3 were also studied by solid-state ^{31}P MAS NMR spectroscopy. Second-order ^{31}P–$^{79,81}Br$ dipolar coupling effects were observed in the ^{31}P MAS NMR spectrum of Br_3PBBr_3. The molecular structure of Br_3PBBr_3 was determined by X-ray diffraction.

Introduction

As early as 1893 Tarible synthesized the first phosphorus halide–boron halide complex Br_3PBBr_3 from the reaction of PBr_3 and BBr_3 in CS_2.[1] Subsequently, papers have appeared regarding the syntheses of the phosphorus halide–boron halide complexes Cl_3PBBr_3,[2,3] Cl_3PBI_3,[3,4] Br_3PBI_3,[3] I_3PBBr_3,[3,5] I_3PBI_3,[3,5–7] and the di-adduct of P_2I_4 with BBr_3 $P_2I_4{\cdot}2BBr_3$[7] although only elemental analyses, melting points, and the infrared spectra of the adducts I_3PBBr_3, I_3PBI_3, $P_2I_4{\cdot}2BBr_3$.[5,7] were published for the characterization of these species.

In 1978 Terao and co-workers reported nuclear quadrupole resonance (NQR) experiments (^{79}Br and ^{127}I) for the Lewis acid–base complexes X_3PBY_3 (X = Br, I; Y = Br, I).[8] In 1983 the same authors also published Br–P–Br and Br–B–Br bond angles for Br_3PBBr_3, which were derived from an ^{81}Br NQR study.[9] Nevertheless, X-ray structural data for these phosphorus halide–boron halide donor–acceptor complexes were not available in the literature except for the related phosphane–haloboranes Me_3PBY_3 (Y = Cl, Br, I),[10] $(SiMe_3)_3PBY_3$ (Y = Cl, Br)[11] and Ph_3PBBr_3.[12]

Previous work has shown that the donor behavior of phosphorus trihalides depends on the electronegativity of the halogen substituents.[13,14] For the phosphorus trihalides, the order of stability for the 1:1 donor–acceptor complexes with boron trihalides is $PCl_3 < PBr_3 < PI_3$.[3] PF_3 appears to have no donor properties if only σ bonding is considered.[15] The order of stability of the adducts formed from boron trihalides with phosphorus trihalides is $BF_3 < BCl_3 < BBr_3 < BI_3$.[16]

Prior to the study described here these complexes had only been poorly investigated and so we repeated the syntheses and characterized the complexes by Raman and IR spectroscopy. In comparison with the results of density functional theory calculations, the vibrational spectra of these species were studied and a systematic order for assigning the vibrational normal modes was found. The compounds Cl_3PBBr_3, Br_3PBBr_3, I_3PBBr_3, and I_3PBI_3 were studied by ^{31}P MAS NMR. The structure of Br_3PBBr_3 was determined by X-ray diffraction.

Results and Discussion

All the compounds reported here were prepared from the reaction of one equivalent of phosphorus trihalide with one equivalent of the boron trihalide.

We attempted to dissolve the iodine-containing adducts I_3PBBr_3 (**5**) and I_3PBI_3 (**6**) in solvents such as CS_2, CH_2Cl_2, CH_3CN, $CFCl_3$, and SO_2 but found the solubility of these complexes to be very limited. The saturated solution in CS_2 contains essentially only very small amounts of the phosphorus trihalide PI_3 and the corresponding boron trihalide BY_3 (Y = Br, I), as indicated by ^{31}P- and ^{11}B-NMR studies.

In contrast to **5** and **6**, the complexes Cl_3PBBr_3 (**1**), Cl_3PBI_3 (**2**), Br_3PBBr_3 (**3**), and Br_3PBI_3 (**4**) dissolve in CH_2Cl_2 and CS_2. ^{31}P- and ^{11}B-NMR studies showed, besides signals for PX_3 (X = Cl, Br, I) and BY_3 (Y = Cl, Br,

[a] Department of Chemistry, Ludwig-Maximilians-Universität München,
Butenandtstraße 5–13 (Haus D), 81377 Munich, Germany
Fax: (internat.) + 49-(0)89/2180-7492
E-mail: tmk@cup.uni-muenchen.de
[b] Institut für Technische Chemie I, Universität Stuttgart, 70550 Stuttgart, Germany
[+] X-ray structure investigations.

 © WILEY-VCH Verlag GmbH, D-69451 Weinheim, 2000 1434–1948/00/1010–2245 $ 17.50+.50/0

I), resonances for several of the mixed species PX_aY_b and BX_aY_b (a, b = 1, 2; $a \neq b$).

Sublimation of these adducts leads to decomposition into PX_3 (X = Cl, Br, I) and BY_3 (Y = Br, I) and we therefore concluded that all phosphorus halide−boron halide complexes **1**−**6** exist only in the solid state.

In the cases of Br_3PBBr_3 (**3**), I_3PBBr_3 (**5**), and I_3PBI_3 (**6**), sublimation could be used to purify these adducts. For Cl_3PBBr_3 (**1**), Cl_3PBI_3 (**2**), and Br_3PBI_3 (**4**) only decomposition products such as mixed species, halogen and uncharacterized products were observed.

Experimental data for the mixed halogen substituted species (X_3PBY_3, X ≠ Y) showed that halogen exchange only occurs in X_3PBY_3, where Y represents the heavier halogen [temperature for the halogen exchange; Cl_3PBBr_3 (**1**) 35−42 °C, Cl_3PBI_3 (**2**) 0 °C, and Br_3PBI_3 (**4**) room temp.].

Another aim of our investigation was the preparation of $P_2I_4{\cdot}2BBr_3$, a compound that was claimed as being isolated in 1901 by Tarible in the reaction of P_2I_4 with two equivalents of BBr_3.[17] Baudler and Fricke did not succeed in repeating Tarible's work,[18] whereas Cowley et al. claimed to have isolated the compound on the basis of IR data.[5]

The Raman spectrum of the yellow solid, obtained from the reaction of P_2I_4 and BBr_3 in CS_2 according to the literature,[5] displayed unequivocally the Raman lines of I_3PBBr_3 (**5**). The vibrational data are very similar to those obtained by Cowley and Cohen[5] and so it can be assumed that P_2I_4 disproportionates into PI_3 (which forms the observed adduct with BBr_3) and a polymeric iodide $(PI)_n$. The same disproportionation was suggested for the reaction of P_2I_4 with BI_3 resulting in the formation of I_3PBI_3.[5]

Vibrational Spectroscopy

Raman and IR Spectra of X_3PBY_3 (X = Cl, Br, I; Y = Br, I) (1−6)

Table 1 and Table 2 summarize the computed and experimentally observed vibrational frequencies of the compounds **1**−**6** synthesized in this study. Figure 1 shows the Raman spectra of the adducts X_3PBY_3 (**3**: X, Y = Br; **6**: X, Y = I) and Figure 2 the Raman spectra of Cl_3PBBr_3 (**1**), Cl_3PBI_3 (**2**), and I_3PBBr_3 (**5**). The vibrational spectra are in good agreement with our calculations (B3LYP) and allow structural assignments to be made. It should be noted that the computation was carried out for a single, isolated (gas-phase) molecule. There may well be significant differences between gas-phase and solid-state spectra.

The two broad peaks in the Raman spectra of **1**, **3**, and **5** in the range of ca. 700−590 cm^{-1} represent the asymmetric stretching vibration of the BBr_3 unit (ω_1) in the complex. The asymmetric B−I stretching mode (ω_1) can be observed in the Raman spectra of **2**, **4**, and **6** in the range of ca. 650−570 cm^{-1} (broad and weak peaks). In contrast to the Raman spectra, two very intense peaks can be assigned to this vibration in the IR spectrum of **6**. (The adducts **2** and **4** decompose rapidly at room temperature and, for this reason, IR data are not available. Compound **4** was contaminated with disproportionation products and therefore its spectrum is not included in Figure 2.) The asymmetric P−X stretching frequency, ω_3, can be found for X = Cl at 590 cm^{-1} (**1**) and for X = Br at 421 cm^{-1} (**3**). Similarly, the values for the asymmetric stretching mode [ν_4 (E), PX_3] for $OPCl_3$ and $OPBr_3$ are reported to be at 581 and 488 cm^{-1},

Table 1. Calculated and observed vibrational frequencies for Br_3PBBr_3 (**3**) and I_3PBI_3 (**6**)

Br_3PBBr_3 (**3**) Calculation[a]	Raman	IR	I_3PBI_3 (**6**) Calculation[a]	Raman	IR	Assignment
657 (128)	650 (0.5)/ 627 (0.5)	687s/ 652vs/ 626s	565 (64)	592 (0.5)/ 572 (0.5)	591m/ 565s	ω_1, ν_{as} (BX_3)
452 (27)	484 (1)/ 475 (0.5)	472vs	440 (38)	n.o.	422w	ω_2, ν (P−B)
436 (102)	n.o.	421m	359 (77)	389 (3)	384vs	ω_3, ν_{as} (PX_3)
359 (198)	374 (3)	380vs	298 (101)	303 (3)/ 288 (0.5)	329w/ 306s/ 288w	ω_4, ν_s (PX_3), ν (P−B), ν_s (BX_3)
229 (9)	235 (10)	234w	157 (1)	163 (10)		ω_{5a}, ν_s (PX_3), ν (P−B), δ_s (BX_3)
175 (1)	186 (2)		122 (0)	126 (6)		ω_{6a}, δ_s (PX_3), ν (P−B), δ_s (BX_3)
161 (0)	169 (4)		113 (0)	120 (6)		ω_7, δ_{as} (PX_3), δ_{as} (BX_3) (bend)
125 (0)	131 (1)		87 (0)	93 (2)		ω_8, δ_{as} (PX_3), δ_{as} (BX_3) (wag)
92 (0)	102 (4)		70 (0)	75 (1)		ω_9, δ_{as} (PX_3), δ_{as} (BX_3) (wag)
75 (0)	73 (0.5)		64 (0)			ω_{10a}, ν (P−B)
56 (0)			50 (0)			ω_{11}, δ_{as} (PX_3), δ_{as} (BX_3) (wag)
28 (0)			26 (0)			ω_{12} (torsion)

[a] In parentheses: IR intensity [km mol^{-1}].

Table 2. Calculated and observed vibrational frequencies for Cl_3PBBr_3 (**1**), Cl_3PBI_3 (**2**), Br_3PBI_3 (**4**) and I_3PBBr_3 (**5**)

Cl_3P-BBr_3 (**1**) Calculation[a]	Raman	IR	Cl_3P-BI_3 (**2**) Calculation[a]	Raman	Br_3P-BI_3 (**4**) Calculation[a]	Raman	I_3P-BBr_3 (**5**) Calculation[a]	Raman	IR	Assignment
669 (156)	693 (0.5, br) 671 (0.5, br)	689s	566 (135)	576 (3)	567 (83)	616 (0.5, br) 575 (0.5, br)	673 (101)	656 (0.5, br) 589 (0.5, br)	647sh 597sh	ω_1, ν_{as} (BY_3)
562 (6)	602 (2)	600br	575 (33)	588 (3)	487 (1)	471 (2)	404 (154)	402 (2)	399s	ω_2, ν_s (P–B)
550 (123)	590 (0.5)	588vs	545(100)	n.o.	431 (100)	n.o.	365 (79)	n.o.	361m	ω_3, ν_{as} (PX_3)
410 (232)	463 (4)	465sh	408 (157)	451 (7)	337 (155)	351 (3)	326 (77)	332 (3)	333vs	ω_4, ν_s (PX_3), ν (P–B), ν_s (BY_3)
							224 (9)	221 (7)	219m	ω_{5a}, ν_s (PX_3), ν (P–B), δ_s (BY_3)
288 (4)	301 (10)	302m	281 (18)	281 (8)	182 (0)	195 (10)				ω_{5b}, δ_s (PX_3), ν (P–B), ν_s (BY_3)
225 (4)	231 (6)	231m	161 (0)	168 (10)	151 (0)	147 (6)				ω_{6a}, δ_s (PX_3), ν (P–B), δ_s (BY_3)
							125 (2)	141 (10)		ω_{6b}, δ_s (PX_3), ν (P–B)
217 (2)	224 (5)		215 (2)	224 (6)	139 (0)	127 (3)	153 (2)	157 (3)		ω_7, δ_{as} (PX_3), δ_{as} (BY_3) (bend)
158 (0)	168 (1)/ 164 (1)		141 (0)	150 (5)	104 (0)		99 (0)	109 (3)		ω_8, δ_{as} (PX_3), δ_{as} (BY_3) (wag)
123 (0)	131 (6)		97 (0)	101 (5)	83(0)	88 (4)	73 (0)	83 (3)		ω_9, δ_{as} (PX_3), δ_{as} (BY_3) (wag)
106 (0)	128 (5)				77 (0)					ω_{10a}, ν (P–B)
			103 (0)	114 (3)						ω_{10b}, ν (P–B), δ_{as} (BY_3)
							64 (1)	64 (0.5)		ω_{10c}, δ_s (PX_3), ν (P–B)
69 (0)			62 (0)	71 (1)	53 (0)		47 (0)			ω_{11}, δ_{as} (PX_3), δ_{as} (BY_3) (wag)
38 (0)			44 (0)		30 (0)		26 (0)			ω_{12} (torsion)

[a] In parentheses: IR intensity [km mol^{-1}].

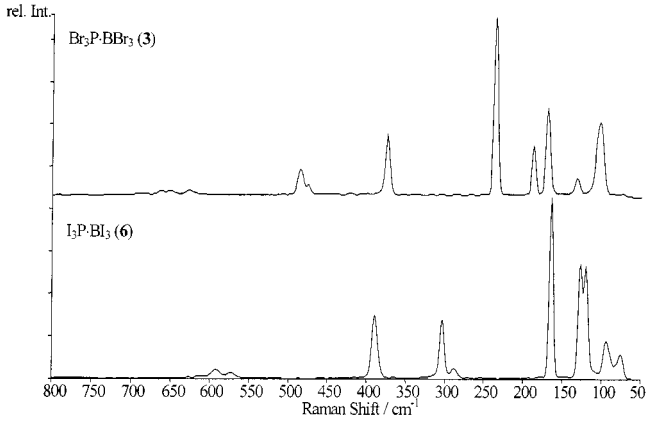

Figure 1. Raman spectra of Br_3PBBr_3 (**3**) and I_3PBI_3 (**6**)

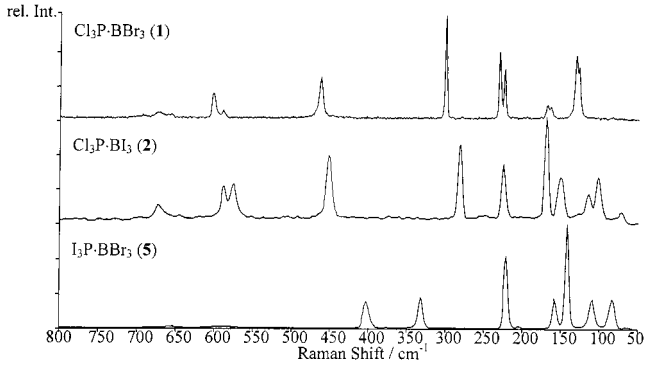

Figure 2. Raman spectra of Cl_3PBBr_3 (**1**), Cl_3PBBr_3 (**2**), and I_3PBBr_3 (**5**)

respectively.[19] The experimental values in the vibrational spectra (IR, Raman) of I_3PBI_3 (**6**) at 387 cm^{-1} and in the IR spectrum of I_3PBBr_3 (**5**) at 361 cm^{-1} can be assigned to the asymmetric stretching vibration of the PI_3 unit (ω_3). Similar vibrational frequencies were reported for the asymmetric stretching modes in the PI_4^+ salts $PI_4^+EI_4^-$ (E = Al, Ga, In)[20,21] at 380 cm^{-1} [ν_3 (T_2), PI_4^+] and in the $P_2I_5^+$ salts $P_2I_5^+EI_4^-$ (E = Al, Ga, In) at 382 cm^{-1}.[22]

Almost purely symmetric P–B stretching vibrations (ω_2) can be observed at 602 (**1**), 588 (**2**), 475 (**3**), 471 (**4**), 402 (**5**), and 422 cm^{-1} (**6**). With heavier halogen substituents the P–B stretching modes are shifted to lower frequencies. The experimental values for the corresponding modes of the related complexes H_3PBY_3 (Y = Cl, Br, I) are found in the range of 679 to 699 cm^{-1}.[23,24]

The assignments of ω_4 to ω_{12} are not as straightforward as those for ω_1 to ω_3. These motions can be described as mixtures of stretches and deformations.

The vibrational mode ω_4, which can be interpreted as a mixture of a P–B stretching mode and symmetric stretching vibrations of the phosphorus trihalide and the boron trihalide units, can be observed and has a similar trend to ω_2: 463 (**1**), 451 (**2**), 377 (**3**), 351 (**4**), 333 cm^{-1} (**5**), and 300 cm^{-1} (**6**).

The mode ω_{5a}, observed as intense peaks in the Raman spectra of **3** (235), **5** (220), and **6** (163), can be described as mixtures of P–B, symmetric PX_3 (X = Cl, Br, I) stretching and symmetric BY_3 (Y = Br, I) deformation modes. A sim-

ilar combination mode, assigned as ω_{5b}, can be observed at 301 (**1**), 281 (**2**), and 195 cm^{-1} (**4**).

The intense Raman frequencies (ω_{6a}), assigned as a combination mode of symmetric deformation modes of the phosphorus halide and boron halide units and a P−B stretching vibration ("umbrella" vibration, $PX_3 + BY_3$ out-of-phase), at 231(**1**), 168 (**2**), 186 (**3**), 147 (**4**), and 126 cm^{-1} (**6**) are reduced to lower wave numbers with heavier halogen substituents.

The bending modes of the PX_3 (X = Cl, Br, I) and BY_3 (Y = Br, I) units, ω_7, can be assigned to peaks with medium intensity in the Raman spectra at 224 (**1**, **2**), 169 (**3**), 127 (**4**), 157 (**5**), and 120 cm^{-1} (**6**).

The normal modes ω_8 to ω_{12} represent fairly complex mixtures of different deformation modes with the exception of the low-lying frequency ω_{10a}, which represents the stretching mode of the entire PX_3 unit towards the BY_3 unit.

Temperature-Dependent Raman Spectra

Br_3PBBr_3 (**3**) decomposes at 61 °C to give a colorless liquid that essentially contains PBr_3 and BBr_3. We recorded the Raman spectra of compound **3** in the temperature region between 20 and 80 °C in steps of 5 °C. Above 60 °C the Raman spectra showed five intense peaks at 383 [ν_1 (A_1), PBr_3], 279 [ν_1 (A_1'), BBr_3], 162 [ν_2 (A_1), PBr_3], 152 [ν_4 (E'), BBr_3], and 115 cm^{-1} [ν_4 (E), PBr_3], which can be assigned to the normal modes of PBr_3 and BBr_3 in the liquid phase.[25,26] The decomposition is reversible. The white Br_3PBBr_3 can be reformed by cooling the liquid to room temperature.

On recording the Raman spectrum of I_3PBBr_3 (**5**) in the temperature range between 20 and 170 °C, we observed that I_3PBBr_3 decomposes into liquid PI_3 {320 [ν_3 (E)], 298 [ν_1 (A_1)], 112 [ν_2 (A_1)], and 82 [ν_4 (E)] cm^{-1}}[27] and BBr_3. Slow cooling of the sample to room temperature led to a yellow solid, which was identified as I_3PBBr_3 with small amounts of I_2 as an impurity. This experiment indicates that halogen exchange does not occur as long as X is heavier than Y (X_3PBY_3).

The melting range of the complex Cl_3PBBr_3 (**1**) is 35−42 °C. The Raman spectrum of the colorless liquid, obtained by heating freshly synthesized Cl_3PBBr_3, shows that at 45 °C the complex decomposes into PCl_3 {514 [ν_3 (E)], 505 [ν_1 (A_1)], 259 [ν_2 (A_1)], and 190 [ν_4 (E)] cm^{-1}},[25] PBr_3 (see above), BCl_3 {472 [ν_1 (A')], 255 [ν_4 (E')] cm^{-1}}[26] and BBr_3 (see above) by halogen exchange. Heating of a sample for 2 d at 70 °C led to a colorless liquid that contained only PBr_3 and BCl_3. It appears that the complex undergoes total halogen exchange. An adduct of Br_3PBCl_3 was not formed after the halogen exchange had occurred, even at temperatures below −130 °C. This result is in agreement with the reports of Holmes,[4] who found that there is no reaction between PBr_3 with BCl_3. Moreover, our density functional calculations show that none of the phosphorus trihalides form 1:1 Lewis acid−base complexes with boron trichloride.

Solid-State ^{31}P-NMR Spectroscopy

The ^{31}P MAS NMR spectra of the compounds I_3PBI_3 (**6**), I_3PBBr_3 (**5**), Br_3PBBr_3 (**3**), and Cl_3PBBr_3 (**1**) are displayed in Figure 3 and the shift data derived from the spectra are summarized in Table 3. The two I_3PBY_3 (Y = Br, I) adducts **5** and **6** show typical spinning side band patterns due to chemical shift anisotropy as observed previously for $PI_4^+EF_6^-$ (E = As, Sb)[20] and $P_2I_5^+EI_4^-$ (E = Al, Ga, In).[22] The central lines of the anisotropy patterns were identified by variation of the spinning frequency and the magnitude of the shift anisotropy δ_{CSA} was estimated by simulation of the side band intensities using the PC program Bruker WINFIT. The spectrum of I_3PBBr_3 (**5**) shows a second weak pattern at δ_{iso} = 237, which originates from PI_3 impurities in the sample.[22]

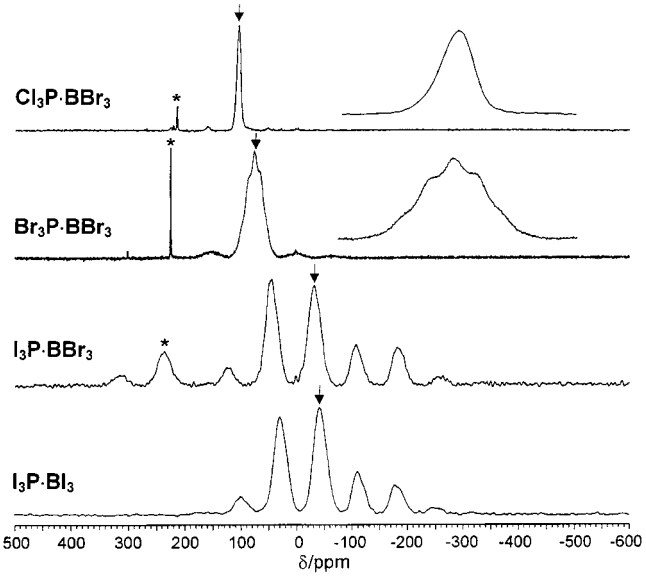

Figure 3. ^{31}P MAS NMR spectra (161.96 MHz) of X_3PBY_3 adducts; the isotropic resonance positions are indicated by arrows, asterisks denote PX_3 impurities (PI_3 in I_3PBBr_3, Br_3P in Br_3PBBr_3, and PCl_3 in Cl_3PBBr_3), all the other lines are spinning side bands; the inserts in the Br_3PBBr_3 and Cl_3PBBr_3 spectra are expanded plots of the resonances centered at δ = 76.9 and 105.3, respectively

Table 3. ^{31}P-NMR isotropic chemical shifts, δ_{iso}, shift anisotropies, δ_{CSA}, and coordination shifts, $\Delta\delta_{coord}$, of X_3PBY_3 compounds (in ppm)

	δ_{iso}	$\Delta\delta_{coord}$[a]	δ_{CSA}[b]
I_3PBI_3 (**6**)	−41.5	−278	−190
I_3PBBr_3 (**5**)	−31.0	−268	−210
Br_3PBBr_3 (**3**)	+76.9	−149	–
Cl_3PBBr_3 (**1**)	+105.3	−110	–

[a] $\Delta\delta_{coord} = \delta_{iso}(X_3P{\cdot}BY_3) - \delta_{iso}(PX_3)$. − [b] $\delta_{CSA} = \delta_{33} - \delta_{iso}$.

The spectra of Br_3PBBr_3 (**3**) and Cl_3PBBr_3 (**1**) exhibit only very weak spinning side bands, indicating small chemical shift anisotropies of the phosphorous atoms in these compounds. Besides the main signals of the adducts (indic-

ated by arrows in Figure 3), narrow lines appear at low field that are attributed to small amounts of PX_3 impurities with X = Br (δ = 226) in Br_3PBBr_3 (**3**) and X = Cl (δ = 214) in Cl_3PBBr_3 (**1**).

Surprisingly, the resonance of Br_3PBBr_3 (**3**) shows an apparent "multiplet" structure (see insert in Figure 3) that is independent of the spinning speed and may formally be simulated by seven overlapping component lines with an equidistant separation of about 1780 Hz. Both the line separation and the intensity distribution rule out a simple explanation in terms of scalar spin-spin coupling between the ^{31}P and the directly bonded $^{79,81}Br$ nuclei [both Br isotopes have a nuclear spin of 3/2, $^1J(^{31}P-^{79,81}Br)$ of 300–380 Hz is reported[28] for PBr_3]. Most probably, the observed "splittings" are caused by second-order effects resulting from dipolar couplings of the ^{31}P with the adjacent $^{79,81}Br$ nuclei, which are not averaged out by magic-angle spinning because of the large quadrupole interaction of the bromine nuclei. Similar effects arising from interactions of ^{31}P with neighboring spin-3/2 quadrupolar nuclei have been observed before for the spin pair $^{31}P-^{63,65}Cu$ in bis(trimethylphosphane) copper(I) nitrate[29] and, more relevant in the context of this study, for $^{31}P-^{35,37}Cl$ in the PCl_4^+ and PCl_6^- ions of solid phosphorus pentachloride.[29] In the latter case, "multiplet" resonances are observed in the ^{31}P MAS NMR spectra that are very similar to the one obtained for Br_3PBBr_3 (**3**). A detailed analysis of this type of second order effect[29] has shown that complex MAS NMR spectra of the spin-1/2 nucleus may arise if the Zeeman interaction of the spin-3/2 nucleus is comparable to, or smaller than, its quadrupole interaction. Under such circumstances the spin states of the quadrupolar nucleus are no longer quantized along the external magnetic field and new terms are introduced in the combined Zeeman-quadrupole Hamiltonian with a different angular dependence than the usual $(3\cos^2\theta - 1)$ term, which is averaged by MAS. The dipolar interaction between the spin-1/2 and the spin-3/2 nucleus may then be reintroduced and gives rise to complex spectral patterns. The quadrupole coupling constant $C_Q = e^2qQ/\mathrm{hbar}$ of the bromine nuclei in the PBr_3 group of Br_3PBBr_3 (**3**) is 426 MHz for ^{81}Br[9] and 518 MHz for ^{79}Br.[8] On comparing these values with the Larmor frequencies of $\nu_L(^{81}Br) = 108$ MHz and $\nu_L(^{79}Br) = 100$ MHz (at 9.4 T), it becomes clear that the quadrupole interaction far exceeds the Zeeman interaction and dipolar coupling may be effective in the ^{31}P MAS NMR spectrum of Br_3PBBr_3 (**3**). To estimate the magnitude of the effect on the spectrum, we calculated the line positions of the ^{31}P multiplets arising from the dipolar coupling with a single Br nucleus for both isotopes following the principles derived in ref.[29] To this end, the parameter $K = -3C_Q/[4S(2S-1)\gamma_S B_o]$ and the dipolar constant $D = (\mu_o/4\pi)\gamma_I\gamma_S\mathrm{hbar}r_{IS}^{-3}$ were calculated, where $C_Q = e^2qQ/\mathrm{hbar}$ is the quadrupole coupling constant; $S = 3/2$, the nuclear spins of $^{79,81}Br$; γ_I and γ_S the magnetogyric ratios of ^{31}P and $^{79,81}Br$, respectively; $B_o = 9.4$ T, the magnetic field used in this study; $r_{IS} = 2.152$ Å, the P–Br distance from Table 4. Values of $K = 1.291$ and 0.986 and $D = 1416$ and 1527 Hz are obtained for the ^{79}Br and ^{81}Br isotopes, respectively. Using these values, the expected spectra were taken from Figure 3 of ref.[29] and are schematically depicted in Figure 4. Theoretically the shape of each resonance is a powder pattern with characteristic divergences and shoulders, but in practice these will be smeared out resulting in broad lines that are approximated by Gaussian lines of equal peak height in Figure 4. It is apparent from this figure that the dipole interaction even with a *single* ^{79}Br or ^{81}Br nucleus already results in splitting of the ^{31}P MAS NMR spectrum into four resonances extending over a spectral range of about 6 kHz, in contrast to the single narrow line to be expected for the unperturbed ^{31}P MAS NMR spectrum. The theoretical spectra of Figure 4 are, of course, not very similar to that observed experimentally for Br_3PBBr_3 (**3**). However, in this molecule the ^{31}P nucleus is coupled to three ^{79}Br and three ^{81}Br nuclei (natural isotopic abundance about 50% each), and further complications by interactions with the ^{11}B nucleus cannot be ruled out. Theoretical calculations of MAS line shapes of spin-1/2 nuclei which interact with three or more spin-3/2 nuclei are difficult and, at present, not feasible. However, such calculations should result in very complex spectral patterns that are not simple superpositions of spectra characterized by interaction with a single quadrupolar nucleus. This conclusion is in full agreement with the experimental findings. It should be noted that, to the best of our knowledge, Br_3PBBr_3 (**3**) is the first example for the observation of second order $^{31}P-^{79,81}Br$ dipolar coupling effects in a ^{31}P MAS NMR spectrum.

Similar dipolar splittings are not observed in the ^{31}P MAS NMR spectra of the I_3PBY_3 (Y = Br, I) and the

Table 4. Theoretical and experimental bond lengths [Å] and angles [°]

		d(PB)	*d*(BY)	*d*(PX)	≤(YBY)	≤(XPX)
BI_3	(calcd.)	–	2.142	–	120.0	–
	(exp.)[a]	–	2.100(1)	–	120.00(2)	–
BBr_3	(calcd.)	–	1.912	–	120.0	–
BCl_3	(calcd.)	–	1.759	–	120.0	–
	(exp.)	–	1.75(2)	–	120.0	–
PI_3	(calcd.)	–	–	2.511	–	103.6
	(exp.)[c]	–	–	2.463(5)	–	102.0(3)
PBr_3	(calcd.)	–	–	2.264	–	101.9
	(exp.)[d]	–	–	2.212(3), 2.216(4)	–	99.0(2), 101.3(2)
PCl_3	(calcd.)	–	–	2.097	–	100.8
	(exp.)[e]	–	–	2.0343(12), 2.0186(23)	–	100.04(7), 100.19(7)
I_3PBI_3	(calcd.)	2.090	2.231	2.481	114.4	105.1
Br_3PBI_3	(calcd.)	2.065	2.232	2.222	114.5	104.3
Cl_3PBI_3	(calcd.)	2.035	2.235	2.049	114.8	103.8
I_3PBBr_3	(calcd.)	2.155	1.984	2.474	115.2	105.8
Br_3PBBr_3	(calcd.)[f]	2.135	1.985	2.200	115.3	104.8
Cl_3PBBr_3	(calcd.)	2.103	1.987	2.048	115.1	102.9

[a] X-ray diffraction: M. A. Ring, J. D. H. Donnay, W. S. Koski, *Inorg. Chem.* **1962**, *1*, 109. – [b] X-ray diffraction: M. Atoji, W. N. Lipscomb, *J. Chem. Phys.* **1957**, *27*, 195. – [c] X-ray diffraction: E. T. Lance, J. M. Haschke, D. R. Peacor, *Inorg. Chem.* **1976**, *15*, 780. – [d] X-ray diffraction: P. R. Enjalbert, J. Galy, *Acta Crystallogr.* **1979**, *B35*, 546. – [e] X-ray diffraction: H. Hartl, M. Rama, *Z. Naturforsch.* **1979**, *34B*, 1035. – [f] See Table 5 for experimental data.

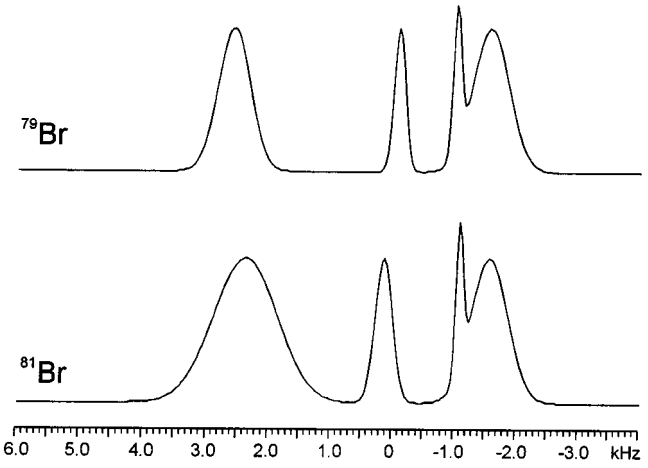

Figure 4. Schematic presentation of theoretical ^{31}P MAS NMR spectra resulting from second-order dipolar splittings with a single ^{81}Br and ^{79}Br nucleus (see text); the frequency scale is relative to the unperturbed ^{31}P resonance at 0 kHz

Cl_3PBBr_3 (**1**) compounds. ^{127}I has a nuclear spin of $S = 5/2$ and a very large C_Q [1931 MHz in I_3PBBr_3 (**5**)[8]] but no theoretical treatment of the dipolar interaction between spin-1/2 and spin-5/2 nuclei has been available so far. Since ^{35}Cl also has $S = 3/2$, the same calculations as considered above for Br_3PBBr_3 (**3**) were carried out for Cl_3PBBr_3 (**1**). The use of $C_Q = 60$ MHz[31] and $\nu_L = 39.2$ MHz for the ^{35}Cl nucleus and $r_{P-Cl} = 1.9$ Å results in the values $K = 0.383$ and $D = 668$ Hz. The theoretical spectrum derived from the data in Figure 3 of ref.[29] consists of two resonance lines that are 380 and 250 Hz wide and are separated by about 750 Hz. Considering the experimental line width of about 1400 Hz, these splittings cannot be resolved, which explains the observation of a single but slightly asymmetric resonance in the ^{31}P MAS NMR spectrum of Cl_3PBBr_3 (**1**) (Figure 3).

On complexing the phosphorus halide molecules with the boron halide the ^{31}P resonance is shifted significantly to higher field, the related "coordination shifts" $\Delta\delta_{coord} = \delta(X_3PBY_3) - \delta(PX_3)$ are summarized in Table 3. The upfield shift is largest for I_3PBI_3 (**6**) and decreases for the X_3PBBr_3 complexes in the order X = I > Br > Cl. However, the coordination shifts do not reflect the increasing charge transfer from the PX_3 donor to the BBr_3 acceptor groups (X = Cl > Br > I) and the concomitant increase of the ionicity of the P−X bonds in these compounds. The coordination shifts, on the other hand, have to be attributed to an increase of the heavy-atom effect at the four-coordinated phosphorus atom in the X_3PBY_3 complexes due to the increased s-character in the P−X bond.[20] Moreover, theoretical studies of NMR chemical shifts revealed that the chemical shift is largely determined by the topology of the electron density distribution at the atom rather than by its partial charge.[32]

Structure

Selected structural data for all X_3PBY_3 adducts (X = Cl, Br, I; Y = Br, I) and monomers are summarized in Table 4. The molecular structures of all species were fully optimized at the B3LYP level. Most of the P−B adducts were shown to possess stable minima at the B3LYP level (no imaginary frequencies), whereas a stable minimum could not be found for any of the X_3PBCl_3 adducts. All adducts possess C_{3v} symmetry with a staggered orientation of the BX_3 and PY_3 fragments. All structural parameters are in good agreement with those of other covalent P−B adducts.[10,11,12]

It should be noted, that the structures of such weakly bound systems may differ considerably between gas phase and the solid state.[33]

Br_3PBBr_3 (**3**, Figure 5) crystallizes in the orthorhombic space group *Pnma* with $Z = 4$. Single-crystal X-ray structure determination showed that the skeletal atoms of this molecule possess a slightly distorted C_{3v} symmetry with a staggered conformation. The P−B bond length was found to be 2.01(2) Å, which is significantly longer than in the corresponding phosphane−haloborane adducts R_3PBBr_3 (R = Me,[10] Ph,[12] $SiMe_3$[11]) and corresponds to a bond order of less than 1. This situation can be explained by the greater electron transfer within Me_3PBI_3 due to the positive inductive effect of the methyl groups, whereas in case of Br_3PBBr_3 and all the other X_3PBY_3 adducts the halogen Y decreases the donor strength of the P atom. In addition, the LP(Y) → σ*(BP) donor-acceptor interactions account for longer B−P distances and introduce a small amount of B−Y π bonding, which results in shorter B−Y distances.

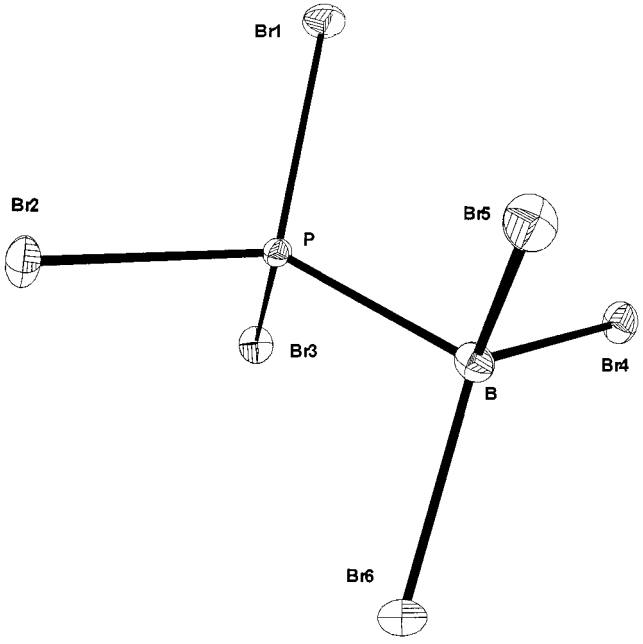

Figure 5. ORTEP plot of Br_3PBBr_3 (**3**)

Table 5 shows the comparison of bond lengths and bond angles of Br_3PBBr_3 (**3**) and the related phosphorus−boron adducts. The X-ray crystal data of **3** confirm that the Br−P−Br and Br−B−Br bond angles are significantly different from the experimental bond angles reported for Br_3PBBr_3 in a ^{81}Br NQR study.[9] The angles and B−Y and P−X distances in all adducts do not change much in the

different X_3PBY_3 species. However, there are more pronounced differences in the B−P distances.

Table 5. Selected bond lengths [Å] and angles [°] for Br_3PBBr_3 (**3**)

P−B[a]	2.01(2)	B−Br(4)[b]	1.96(2)
P−Br(1)	2.151(4)	B−Br(5)	1.99(1)
P−Br(2)	2.152(3)	B−Br(6)	1.99(1)
P−Br(3)	2.152(3)		
Br(1)−P−Br(2)[c]	106.6(1)	B−P−Br(1)	114.0(6)
Br(1)−P−Br(3)	106.6(1)	B−P−Br(2)	110.9(3)
Br(2)−P−Br(3)	107.5(2)	B−P−Br(3)	110.9(3)
Br(4)−B−Br(5)[d]	114.7(6)	Br(4)−B−P	104.1(8)
Br(4)−B−Br(6)	114.7(6)	Br(5)−B−P	104.2(6)
Br(5)−B−Br(6)	113.2(9)	Br(6)−B−P	104.2(6)

[a] Cf.: *d*(P−B) = 1.998(21) [$(SiMe_3)_3P{\cdot}BBr_3$];[11] 1.924(12) [$Me_3P{\cdot}BBr_3$];[10] 1.988(10) [$Ph_3P{\cdot}BBr_3$].[12] − [b] Cf.: *d*(B−Br) = 1.995(20) to 2.035(20) [$(SiMe_3)_3P{\cdot}BBr_3$];[11] 2.016(10) to 2.025(6) [$Me_3P{\cdot}BBr_3$];[10] 1.978(10) to 2.013(9) [$Ph_3P{\cdot}BBr_3$].[12] − [c] Cf.: ^{81}Br NQR study, <(Br−P−Br) = 107.0 (±0.1) to 109.1 (±0.3);[9] 108.3(9) to 109.7(10) [$(SiMe_3)_3P{\cdot}BBr_3$];[11] 110.0(5) to 110.6(4) [$Me_3P{\cdot}BBr_3$].[10] − [d] Cf.: ^{81}Br NQR study, <Br−B−Br = 111.2 (±0.1) to 111.5 (±0.1).[9]

The calculated B−Y bond lengths in all adducts are much longer than in the isolated BY_3 moieties. Upon complexation, the lengthening of the B−Y bonds increases from BBr_3 to BI_3 adducts. This can be attributed to the greater π bonding character of the B−Y bonds in the isolated BY_3 molecules than in the adducts which increases from I to Cl.

Upon coordination, the lone pair electrons on the P atom are partially donated, resulting in a shrinking of the P−X bonds (compared to the PX_3 fragment) and opening of the X−P−X angles. This shortening is related to the dramatically increasing "s" character in the P−X bond of the complex [e.g. $h_P(PI_3) \approx sp^{17.20}$ vs. $h_P(I_3PBI_3) \approx sp^{2.71}$].

Additionally, the more electronegative Cl ligands in PCl_3 lead to better orbital overlap due to orbital contraction and, therefore, to a better electron transfer and a shorter B−P bond length. This feature is in agreement with Durig and Shen's finding for the H_3PBH_3 (1.943 Å) and F_3PBH_3 (1.836 Å) complexes.[34]

Conclusion

The structure and the vibrational normal modes of phosphorus halide−boron halide complexes Cl_3PBBr_3 (**1**), Cl_3PBI_3 (**2**), Br_3PBBr_3 (**3**), Br_3PBI_3 (**4**), I_3PBBr_3 (**5**), and I_3PBI_3 (**6**) have been calculated, discussed and compared with the experimental values. Vibrational assignments have been made on the basis of the Raman and IR spectra in comparison with computational results. Our calculations agree reasonably with the experimental data.

Temperature-dependent Raman experiments indicate that halogen exchange cannot be observed as long as X is heavier than Y in X_3PBY_3 (e.g. in I_3PBBr_3). In contrast, halogen exchange occurs when Y is heavier (e.g. within Cl_3PBBr_3).

The adducts Cl_3PBBr_3 (**1**), Br_3PBBr_3 (**3**), I_3PBBr_3 (**5**), and I_3PBI_3 (**6**) have been characterized by solid-state ^{31}P MAS NMR spectroscopy. The solid-state ^{31}P MAS NMR spectra reveal an increasing upfield shift for the X_3PBY_3 complexes in the order X = Br < I and Y = Cl < Br < I due to heavy-atom effects. The ^{31}P MAS NMR of Br_3PBBr_3 (**3**) represents the first example of second order $^{31}P-^{79,81}Br$ dipolar coupling effects.

All P−B bond lengths are rather long due to destabilizing donor−acceptor interactions. The increasing s character of the P−X bond in the complexes results in a opening of the X−P−X angles.

Adduct structures that represent true minima were found for all X_3PBY_3 species except for the cases where BCl_3 was the Lewis acid.

Experimental Section

General Remarks: All compounds reported here are moisture-sensitive, some extremely so, and decompose within a few seconds if exposed to the atmosphere. Consequently, strictly anaerobic and anhydrous conditions were employed for their synthesis. Any subsequent manipulations were carried out inside a dry-box under dry nitrogen. PBr_3, PCl_3, PI_3, BBr_3, and BI_3 (all Aldrich) were used as received. CS_2 was refluxed with P_4O_{10} and distilled before used. − ^{31}P-NMR spectra were measured at 161.96 MHz with a BRUKER MSL-400 NMR spectrometer under magic-angle-spinning (MAS) conditions. A standard double-bearing MAS probe for 4-mm rotors was used with spinning frequencies up to 12 kHz. Single-pulse acquisition with 1-μs pulse width (corresponding to 25° flip angle) and 5-s pulse repetition was applied. The samples were filled in 4-mm zirconia rotors under nitrogen in a glove box. The spectra were referenced to 85% aqueous phosphoric acid. Simulations of spectra were carried out with the PC program WINFIT from the BRUKER WINNMR software package. − Raman spectra of powdered solid samples contained in glass capillary tubes were obtained with with a Perkin−Elmer 2000 NIR spectrometer in the range 800−50 cm^{-1}. The low-temperature spectra were recorded using a Ventacon low-temperature cell and the high-temperature spectra were obtained using a Ventacon high-temperature cell. − IR spectra of Nujol mulls between CsI plates were taken in the range 800−200 cm^{-1} with a Nicolet 520 FT IR spectrometer. − For the determination of decomposition points, samples were heated in sealed glass capillaries in a Büchi B450 instrument.

Cl_3PBBr_3 (1): Cl_3PBBr_3 was prepared by addition of BBr_3 (1.56 g, 6.23 mmol) to PCl_3 (1.57 g, 11.40 mmol) with stirring at −40 °C. A colorless solid formed immediately. After warming the mixture to −30 °C, the remaining PCl_3 was removed under dynamic vacuum. − Yield: 1.50 g (44%) of a colorless solid, m.p. 35−42 °C (decomp.).

Cl_3PBI_3 (2): Cl_3PBI_3 was prepared by addition of PCl_3 (1.57 g, 11.40 mmol) to BI_3 (0.92 g, 2.35 mmol) with stirring at −40 °C. A colorless solid formed immediately. After warming the mixture to −30 °C, the remaining PCl_3 was removed under dynamic vacuum. − Yield: 1.30 g (95%) of a colorless solid, m.p. 0 °C (decomp.). − *Note:* Compound **2** undergoes halogen exchange above 0 °C, as indicated by a change in color from colorless to yellow. The impurity at 673 cm^{-1} in the Raman spectrum of **2** is due to this halogen exchange.

Br_3PBBr_3 (3): Br_3PBBr_3 was prepared by addition of PBr_3 (1.66 g, 6.13 mmol) in CS_2 to CS_2 solutions of BBr_3 (1.76 g, 7.03 mmol) with stirring at −40 °C. A colorless solid formed immediately. After

stirring for 15 min, the solid was filtered off. Traces of the solvent were removed under dynamic vacuum at room temperature. − Yield: 2.64 g (83%) of a colorless solid, m.p. 61 °C (decomp.).

Br_3PBI_3 (4): Br_3PBI_3 was prepared by addition of PBr_3 (0.42 g, 1.55 mmol) in CS_2 to CS_2 solutions of BI_3 (0.61 g, 1.55 mmol) with stirring at −40 °C. A yellow solid formed immediately. After stirring for 15 min, the solid was filtered off. Traces of the solvent were removed under dynamic vacuum at room temperature. − Yield: 0.92 g (90%) of a yellow solid, m.p. 150 °C (decomp., halogen exchange).

I_3PBBr_3 (5): I_3PBBr_3 was prepared by addition of PI_3 (1.63 g, 3.95 mmol) in CS_2 to CS_2 solutions of BBr_3 (0.99 g, 3.95 mmol) with stirring at −40 °C. A yellow precipitate formed immediately. After stirring for 15 min, the precipitate was isolated by filtering twice and washing with CS_2. Traces of CS_2 were removed under dynamic vacuum at room temperature. − Yield: 2.90 g (51%) of a yellow solid, m.p. 158−160 °C (decomp.).

I_3PBI_3 (6): I_3PBI_3 was prepared by addition of PI_3 (1.24 g, 3.01 mmol) in CS_2 to CS_2 solutions of BI_3 (1.17 g, 3.01 mmol) with stirring at room temperature. An orange precipitate formed immediately. After stirring for 15 min, the precipitate was isolated by filtration and washed with CS_2 until the filtrate was colorless. Traces of CS_2 were removed under dynamic vacuum at room temperature. − Yield: 1.88 g (78%) of an orange solid, m.p. > 250 °C (decomp.).

Computational Methods: The structure and vibrational data for the phosphorus halide−boron halide complexes **1**−**6** were calculated using the density functional theory with the program package Gaussian 94.[35] For P and B a standard 6-31G(d) basis set was used and for I, Br, and Cl a quasi-relativistic pseudopotential (I: ECP46MWB; Br: ECP28MWB; Cl: ECP10MWB)[36] and a (5s5p1d)/[3s3p1d]-DZ+P basis set.[37] The computations were carried out at the DFT level using the hybrid method B3LYP, which includes a mixture of Hartree−Fock exchange with DFT exchange-correlation. Becke's 3 parameter functional, where the non-local correlation is provided by the LYP expression (Lee, Yang, Parr correlation functional), was used as implemented in Gaussian 94. For a concise definition of the B3LYP functional see ref.[38]

Crystal Structure Analysis of 3: BBr_6P, M = 521.24, crystal size: 0.40 × 0.10 × 0.10 mm, colorless prism, orthorhombic, space group *Pnma*, a = 12.195(3), b = 11.054(2), c = 7.053(1) Å, V = 850.8(4) Å^3, Z = 4, $d_{calcd.}$ = 3.641 Mg m^{-3}, μ = 25.418 mm^{-1}, $F(000)$ = 920. Siemens P4 diffractometer with CCD area detector, scan type: hemisphere, Mo-K_α, (λ = 0.71073 Å), T = 185 K, 2θ range = 6.68−55.20° in $-15 \le h \le 15$, $-11 \le k \le 11$, $-9 \le l \le 9$, reflections collected: 5006, independent reflections: 962 (R_{int} = 0.0634), observed reflections: 733 [$F > 4\sigma(F)$], T_{max}/T_{min} = 0.1854/0.0350. Structure solution and refinement program: SHELXL-97,[39] direct methods, data-to-parameter ratio: 22.4:1 (17.0:1 [$F > 4\sigma(F)$]), final R indices [$F > 4\sigma(F)$]: $R1$ = 0.0842, $wR2$ = 0.2131, $R1$ = 0.0976, $wR2$ = 0.2204 (all data), GOF on F^2 = 1.123, largest and mean Δ/σ: 0.000, 0.000, largest difference peak/hole: 2.666, −3.458 e Å^{-3}. − Further details of the crystal structure investigation may be obtained from the Fachinformationszentrum Karlsruhe, D-76344 Eggenstein-Leopoldshafen, Germany, on quoting the depository number CSD-41194.

Acknowledgments

We gratefully acknowledge the support of the Fonds der Chemischen Industrie and the University of Munich. We also wish to thank Mr. G. Spieß for his help with the Raman experiments and the Leibniz Rechenzentrum for a generous allocation of CPU time. In addition we would like to thank Prof. Martin Kaupp for valuable discussions. We would also like to thank both referees for helpful comments.

[1] J. Tarible, *C. R. Acad. Sci.* **1893**, *116*, 1521.
[2] E. Wiberg, K. Schuster, *Z. Anorg. Allg. Chem.* **1933**, *213*, 94.
[3] A. F. Armington, J. R. Weiner, G. H. Moates, *Inorg. Chem.* **1966**, *5*, 483.
[4] R. R. Holmes, *J. Inorg. Nucl. Chem.* **1960**, *12*, 266.
[5] A. H. Cowley, S. T. Cohen, *Inorg. Chem.* **1965**, *4*, 1200.
[6] R. F. Mitchell, J. A. Bruce, A. F. Armington, *Inorg. Chem.* **1964**, *3*, 915.
[7] G. W. Chantry, A. Finch, P. N. Gates, D. Steele, *J. Chem. Soc. A* **1966**, 896.
[8] H. Terao, T. Okuda, H. Negita, *Bull. Chem. Soc. Jpn.* **1978**, *51*, 710.
[9] H. Terao, M. Fukura, T. Okuda, H. Negita, *Bull. Chem. Soc. Jpn.* **1983**, *56*, 1728.
[10] D. L. Black, R. C. Taylor, *Acta Crystallogr.* **1975**, *B31*, 1116.
[11] M. S. Lube, R. L. Wells, P. White, *Inorg. Chem.* **1996**, *35*, 5007.
[12] F. Weller, M. Möhlen, K. Dehnicke, *New Cryst. Struct.* **1997**, *212*, 159.
[13] D. S. Payne, *Quart. Rev.* **1961**, *15*, 173.
[14] R. R. Holmes, *J. Chem. Educ.* **1963**, *40*, 125.
[15] cf. R. W. Parry, T. C. Bissot, *J. Am. Chem. Soc.* **1956**, *78*, 1524.
[16] D. Cook, *Can. J. Chem.* **1963**, *41*, 522.
[17] J. Tarible, *C. R. Acad. Sci.* **1901**, *132*, 204.
[18] M. Baudler, G. Fricke, *Z. Anorg. Allg. Chem.* **1963**, *319*, 212.
[19] M. L. Dewaulle, F. Francois, *C. R. Acad. Sci.* **1945**, *220*, 817.
[20] M. Kaupp, Ch. Aubauer, G. Engelhardt, T. M. Klapötke, O. L. Malkina, *J. Chem. Phys.* **1999**, *110*, 1729.
[21] Ch. Aubauer, T. M. Klapötke, A. Schulz, *Int. J. Vibr. Spectrosc.* **1999**, *3*, 4; (http://www.ijvs.com/volume3/edition2/section4.htm).
[22] Ch. Aubauer, G. Engelhardt, T. M. Klapötke, A. Schulz, *J. Chem. Soc., Dalton Trans.* **1999**, 1729.
[23] J. R. Durig, S. Riethmiller, V. F. Kalasinsky, J. D. Odom, *Inorg. Chem.* **1974**, *13*, 2729.
[24] J. D. Odom, S. Riethmiller, J. D. Witt, J. R. Durig, *Inorg. Chem.* **1973**, *12*, 1123.
[25] R. J. H. Clark, D. M. Rippon, *J. Mol. Spectrosc.* **1974**, *72*, 58.
[26] R. J. H. Clark, P. D. Mitchell, *J. Chem. Phys.* **1972**, *56*, 2225.
[27] H. Stammreich, R. Forneris, Y. Tavares, *J. Chem. Phys.* **1956**, *25*, 580.
[28] *Multinuclear NMR* (Ed.: J. Mason), Plenum Press, New York, **1989**, p. 454.
[29] E. M. Menger, W. S. Veeman, *J. Magn. Reson.* **1982**, *46*, 257.
[30] R. K. Harris, A. Root, *Mol. Phys.* **1989**, *66*, 993.
[31] *Nuclear Quadrupole Resonance in Chemistry* (Eds.: G. K. Semin, T. A. Babushkina, G. G. Yakobsen), Wiley, **1975**, p. 473.
[32] [32a] U. Pidun, M. Stahl, G. Frenking, *Chem. Eur. J.* **1996**, *2*, 869. − [32b] W. Kutzelnigg, U. Fleischer, M. Schindler, *NMR* **1990**, *23*, 165.
[33] [33a] R. Jürgens, J. Almlöf, *Chem. Phys. Lett.* **1991**, *276*, 263. − [33b] R. Ahlrichs, M. R. Bär, M. Häser, E. Sattler, *Chem. Phys. Lett.* **1991**, *184*, 353.
[34] J. R. Durig, Z. Shen, *J. Mol. Struct. (Theochem)* **1997**, *397*, 179.
[35] M. J. Frisch, G. W. Trucks, H. B. Schlegel, P. M. W. Gill, B. G. Johnson, M. A. Robb, J. R. Cheeseman, T. Keith, G. A. Peterson, J. A. Montgomery, K. Raghavachari, M. A. Al-Laham, V. G. Zakrzewski, J. A. Ortiz, J. B. Foresman, C. Y. Peng, P. Y. Ayala, W. Chen, M. W. Wong, J. L. Andres, E. S. Replogle, R. Gomperts, R. L. Martin, D. J. Fox, J. S. Binkley, D. J. Defrees, J. Baker, J. P. Stewart, M. Head-Gordon, C. Gonzales, J. A. Pople, *Gaussian 94*, Revision B.2, Gaussian, Inc., Pittsburgh, **1995**.
[36] [36a] P. Schwerdtfeger, M. Dolg, W. H. E. Schwarz, G. A. Bowmaker, P. D. W. Boyd, *J. Chem. Phys.* **1989**, *91*, 1762. − [36b] A.

Bergner, M. Dolg, W. Kuechle, H. Stoll, H. Preuss, *Mol. Phys.* **1993**, *80*, 1431.
[37] M. Kaupp, P. v. R. Schleyer, H. Stoll, H. Preuss, *J. Am. Chem. Soc.* **1991**, *113*, 1602.
[38] [38a] C. W. Bauschlicher, H. Partridge, *Chem. Phys. Lett.* **1994**, *231*, 277. − [38b] A. D. Becke, *J. Chem. Phys.* **1993**, *98*, 5648. − [38c] A. D. Becke, *Phys. Rev. A* **1988**, *38*, 3098. − [38d] C. Lee, W. Yang, R. G. Parr, *Phys. Rev. B* **1988**, *37*, 785. − [38e] S. H. Vosko, L. Wilk, M. Nusair, *Can. J. Phys.* **1980**, *58*, 1200. −
[39] G. M. Sheldrick, *SHELXL-97*, Program for Crystal Structure Determination, University of Göttingen, Germany, **1997**.

Received March 17, 2000
[I00099]